ELSEVIER

Science and Technology of Advanced Materials 6 (2005) 704–711

SCIENCE AND TECHNOLOGY OF ADVANCED MATERIALS

www.elsevier.com/locate/stam

# Fabrication of piezoelectric laminate for smart material and crack sensing capability

Sirirat Rattanachan[a,*], Yukio Miyashita[b], Yoshiharu Mutoh[b]

[a]*Institute of Engineering, Suranaree University of Technology, 111 University Avenue, Nakhon Ratchasima 30000, Thailand*
[b]*Department of Mechanical Engineering, Nagaoka University of Technology, 1603-1 Kamitomioka, Nagaoka-shi 940-2188, Japan*

Received 12 October 2004; revised 23 May 2005; accepted 8 June 2005
Available online 24 August 2005

**Abstract**

Piezoelectric laminate composite has been successfully fabricated as a smart material by a spark plasma sintering process. Fully or nearly fully dense $BaTiO_3$/MgO (pre-sintered)/$BaTiO_3$, $BaTiO_3$/MgO with 10 vol% $BaTiO_3$/$BaTiO_3$ laminates were sintered at 1300 °C with a holding time of 5 min under a pressure of 35 MPa. From EDS analysis, no reaction between $BaTiO_3$ and MgO layers was observed along the interface. Effects of cycle stress and stress intensity factor on the voltage response of the proposed laminates were investigated for confirmation of a crack detecting capability. The resultant relationship between crack length and voltage response range clearly showed that the proposed laminates have a crack sensing capacity.


*Keywords:* Smart material; Piezoelectric; Laminate; Spark plasma sintering; Fatigue; Crack sensing

## 1. Introduction

One of the major concerns of ceramic materials is the susceptibility to fracture, which may occur during manufacture, service or maintenance. Application of service loading can often induce serious damage to ceramics such as cracking. Although such damage is barely visible, it can severely degrade the mechanical properties and the load carrying capability of the structure. Safety and damage-tolerance of ceramic structures are also important. Effective maintenance and continuous health monitoring of ceramic structures not only reduce the life-cycle costs but also improve safety. Piezoelectric materials have a property of converting mechanical energy to electrical energy and vice versa [1]. Therefore, these materials can be used as sensors and/or actuators [2]. In the passive approach, they are bonded or embedded in the sensing devices in order to monitor ultrasonic or acoustic-ultrasonic waves, as ultrasonic detection probe and acoustic emission probe. Damage in a structure can be identified by a change of the response signal by using these probes.

Self-monitoring materials constitute a class of structural materials, which are intrinsically smart. The factors for structural health monitoring and controlling are strain and damage. These materials are self-monitoring because they can reveal problems before the failure occurs.

In recent years, new ceramic matrix composites with piezoelectric secondary phase have been developed [3–5]. High fracture toughness of $BaTiO_3$–$Al_2O_3$ composite sintered by a spark plasma sintering method has been obtained, compared to the monolithic $Al_2O_3$ [6]. To determine the crack sensing capability of the new ceramic matrix composites with piezoelectric secondary phase, the voltage response under fatigue test of the poled MgO-based composite with 10 mol% $BaTiO_3$ (denoted as 90M10B) was determined as shown in Fig. 1. It can be seen from the figures that the voltage response was very low and not related to the applied compressive cyclic stress. It indicates that the ceramic matrix composites with piezoelectric secondary phases are not capable of monitoring strain or damage. It was beneficial to fabricate the laminates with piezoelectric $BaTiO_3$ as a self-damage sensing material in this study.

Spark plasma sintering (SPS) was used as a fast densification method because it was considered to be

* Corresponding author. Tel.: +66 44 224489; fax: +66 44 224220.
*E-mail address:* sirirat.b@sut.ac.th (S. Rattanachan).

1468-6996/$ - see front matter © 2005 Elsevier Ltd. All rights reserved.
doi:10.1016/j.stam.2005.06.002

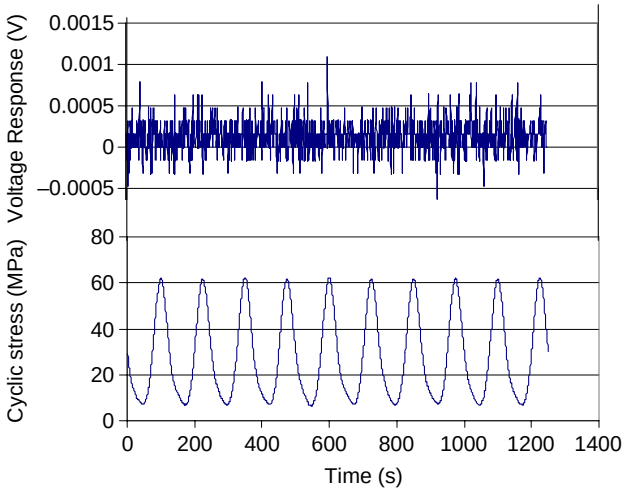


Fig. 1. The voltage response and cyclic stress for the poled piezoelectric-particle-dispersed composite (90M10B) under fatigue test.

suitable for fabricating the laminated and functionally graded composites [6,7]. It is possible to sinter by SPS at a lower temperature and for a shorter duration. In the present study, piezoelectric laminates were fabricated by means of SPS. Detailed characterization of the piezoelectric laminates was carried out. Crack sensing ability of the proposed composite was also investigated during a fatigue test.

## 2. Experimental procedure

### 2.1. Sample preparation

The starting materials were $BaTiO_3$ powder (Ba/Ti atomic ratio: 1, average particle size: 0.5 μm, Sakai chemical industrial Co. Ltd.) and high purity MgO powder (99.99% MgO, analytical grade and average particle size of 2 μm). $BaTiO_3$/90MgO10$BaTiO_3$/$BaTiO_3$ laminates were fabricated as follows: 10 vol% $BaTiO_3$ and 90 vol% MgO powders (denoted as 90M10B) were mixed by alumina ball milling with alumina balls in ethanol for 24 h. The mixed slurry was dried by a rotary evaporator, and was then milled again and sieved through a 150 μm mesh screen. The laminated samples consist of three layers with a middle layer of MgO or MgO-based composite as well as outer layers of $BaTiO_3$. The thicknesses of the middle layer and the outer layers were 2 and 1 mm, respectively. The mixtures with the corresponding compositions were stacked into a die layer by layer and sintered by using a SPS machine under an applied load of 38 MPa in vacuum. The temperature was increased at a rate of 100 °C/min up to the sintering temperature. After holding for 5 min at the sintering temperature, the d.c. power of the SPS machine was shut off to let the sintered sample cool rapidly to 600 °C for 30 min. During sintering, the shrinkage behavior was observed by monitoring the displacement of the sample along the pressing direction.

$BaTiO_3$/MgO/$BaTiO_3$ laminate was difficult to sinter due to a large difference of sintering temperature between MgO and $BaTiO_3$ materials. The following two-step sintering method was adopted for fabrication: the monolithic MgO layer was pre-shaped by sintering at 1300 °C, and then the $BaTiO_3$ powders were stacked on both sides of the MgO layer and sintered at 1100 °C again.

### 2.2. Characterization

The density of the samples was measured according to Archimedes' principle. The microstructure was investigated on a scanning electron microscope, and the chemical composition near the interface region was determined by using an energy-dispersive spectrometer (EDS). In addition, an X-ray diffractrometer with Cu Kα radiation generated at 30 kV and 30 mA was used for determining the phases of each layer.

### 2.3. Testing procedure

The sintered samples were cut into rectangular bar specimens with a diamond saw. The specimen surfaces were then ground and polished with 600# SiC abrasive and fine diamond paste of 0.2 μm to yield a mirror-like surface suitable for indentation. The final dimensions of the specimen were 4×3×20 mm, as shown in Fig. 2.

Two longitudinal surfaces (surface on side of 20×1 mm) on the $BaTiO_3$ layers were coated with silver paste for poling. Two conductive wires for applying electrical voltage were attached onto both surfaces of the electrode by soldering. The electric field of 500–600 V/mm was applied perpendicular to the laminate direction, as schematically shown in Fig. 2. A crack was introduced on the polished surface of the outer $BaTiO_3$ layer (surface on side of 20×3 mm) or the middle layer (surface on side of 20×2 mm) by a Vickers indenter.

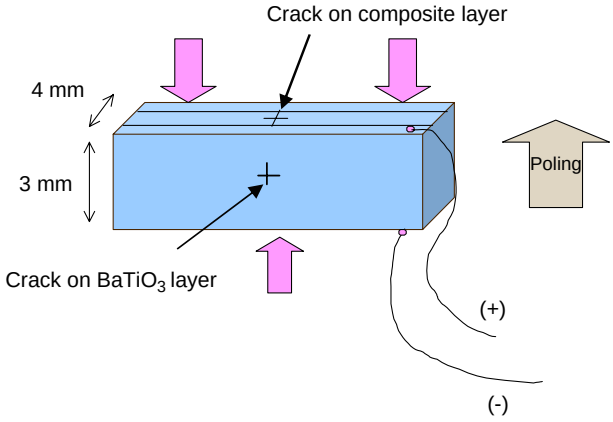


Fig. 2. Schematic set up of the specimen for poling and cyclic loading.

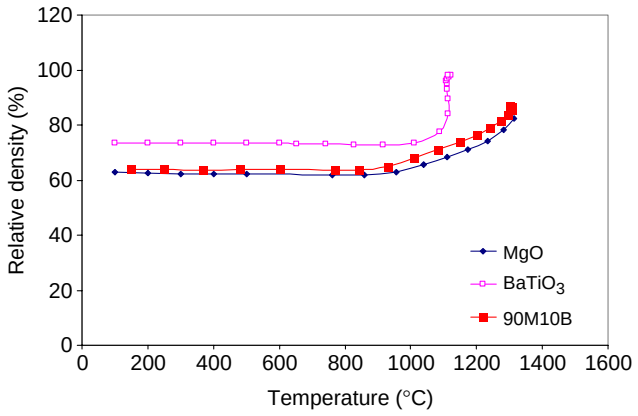


Fig. 3. Sintering behavior of the monolithic $BaTiO_3$, MgO and the composite 90M10B.

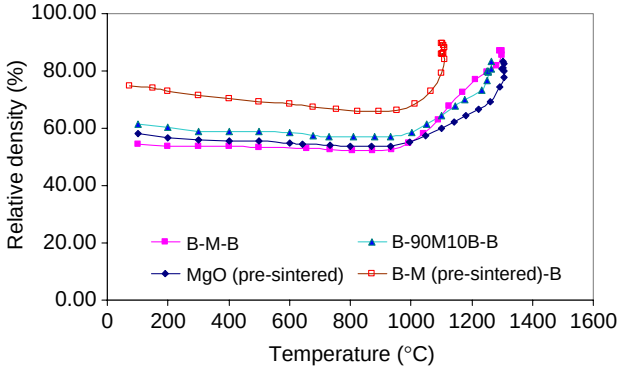


Fig. 4. Sintering behavior of the piezoelectric laminates. (Abbreviation: B/M/B: $BaTiO_3$/MgO/$BaTiO_3$, B/90M10B/B: $BaTiO_3$/90M10B/$BaTiO_3$, B/M. (pre-sintered)/B: $BaTiO_3$/MgO(pre-sintered)/$BaTiO_3$).

The three point bending fatigue test with a span length of 10 mm was performed by using a servo-hydraulic testing machine, where a sinusoidal load with a frequency of 20 Hz and a stress ratio (ratio of minimum and maximum stress to which the sample is subjected) of 0.1 was applied. The fatigue test was conducted to investigate the relationship between the fatigue crack growth rate and the responding output signal of the laminates after poling. During the fatigue test of laminates, variation of output signal through a charge amplifier was recorded with a sampling time of 0.5 ms, as compared with the monolithic $BaTiO_3$.

## 3. Results and discussion

### 3.1. Sintering behavior of bulk materials

The variations in the relative density of the monolithic $BaTiO_3$, MgO and the composite 90M10B during sintering are shown in Fig. 3. $BaTiO_3$ began to shrink at 1100 °C and had a high densification rate before reaching full density at 1120 °C. MgO began to shrink at approximately 950 °C and had a low densification rate. The sintering behavior of 90M10B was similar to that of MgO.

### 3.2. Sintering behavior of laminates

The relationship between the relative density and temperature of $BaTiO_3$/MgO/$BaTiO_3$, $BaTiO_3$/MgO (pre-sintered)/$BaTiO_3$ and $BaTiO_3$/90M10B/$BaTiO_3$ laminates together with that of MgO during sintering are shown in Fig. 4. Two kinds of laminates, $BaTiO_3$/MgO/$BaTiO_3$ and $BaTiO_3$/90M10B/$BaTiO_3$, began to shrink at 1100 °C. The densification rate of $BaTiO_3$/MgO/$BaTiO_3$ was higher than that of $BaTiO_3$/90M10B/$BaTiO_3$.

The sintering behavior of $BaTiO_3$/MgO (pre-sintered) /$BaTiO_3$ laminate is also shown in Fig. 4. $BaTiO_3$/MgO (pre-sintered)/$BaTiO_3$ which began to shrink around 1100 °C and had a high densification rate which was the same as the sintering of monolithic $BaTiO_3$, as shown in Fig. 3.

### 3.3. Microstructure of laminates

The phase of the $BaTiO_3$ layer for the $BaTiO_3$/MgO/$BaTiO_3$ laminate sintered by SPS at 1300 °C for 5 min was analyzed by the X-ray diffraction method. Tetragonal $BaTiO_3$ phase was found, as shown in Fig. 5.

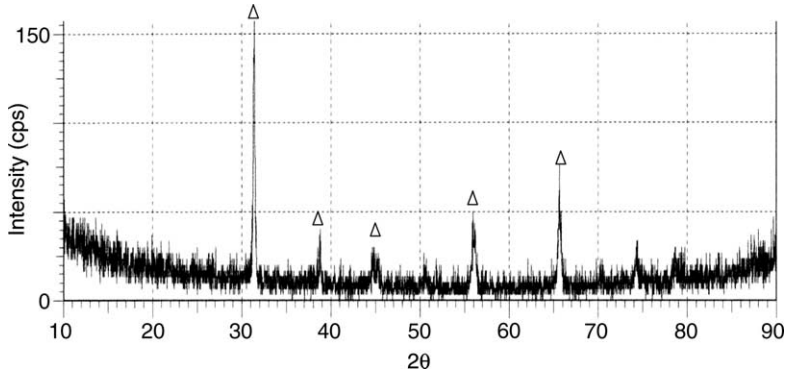


Fig. 5. XRD patterns of the $BaTiO_3$ layer in the $BaTiO_3$/MgO/$BaTiO_3$ laminate sintered at 1300 °C by SPS.

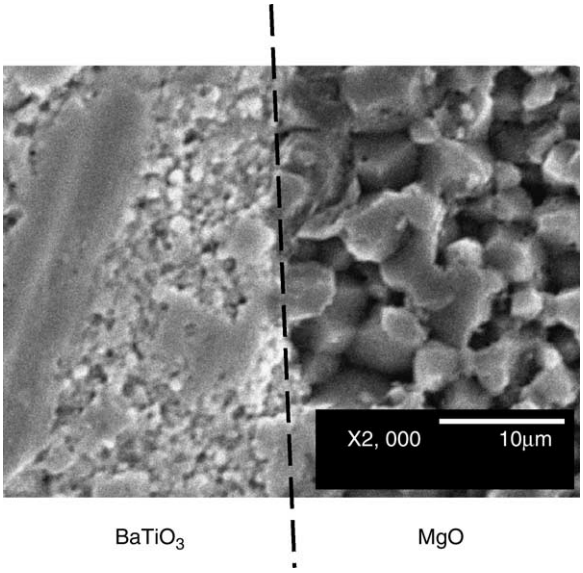


Fig. 6. SEM micrographs of the near interface region of $BaTiO_3$/MgO/$BaTiO_3$ laminate.

A high magnification SEM micrograph of the near interface region of $BaTiO_3$/MgO/$BaTiO_3$ laminate sintered by SPS at 1300 °C is shown in Fig. 6. The average grain sizes of $BaTiO_3$ and MgO were 0.5 and 3–5 μm, respectively. From Fig. 5, peaks, which are indicated by triangles, are 110, 111, 200, 211 and 220 diffractions. From the X-ray pattern, peaks of 200, 211 and 220 diffractions should be split, when the phase is tetragonal phase. Since the small diffraction area on the $BaTiO_3$ layer and the small grain size affected the obtained X-ray pattern, the splitting of these peaks appeared unclear including the noise. It appears that the grain size is strongly related to paraelectric and ferroelectric transformation. When the grain size is below a certain level, the crystallographic cell becomes more and more cubic. Shaikh [8] and co-workers have proposed a model that $BaTiO_3$ ceramics consist of cubic grain boundaries and tetragonal interior grains. The fraction of paraelectric cubic phase increases as the grain size decrease. In this study, composite laminates sintered by SPS consisted of mainly 50 nm grains, resulting in a relative small amount of cubic phase, as similar to the work of Luan W. et al. [9]. In this result, phase analysis showed probably tetragonal and a small amount of cubic phases. However, the $BaTiO_3$ layers showed the piezoelectric effect after polarization.

Scanning electron micrographs of the cross-sections of the $BaTiO_3$/MgO/$BaTiO_3$, $BaTiO_3$/MgO (pre-sintered)/$BaTiO_3$ and $BaTiO_3$/90M10B/$BaTiO_3$ are shown in Fig. 7 (a)–(c), respectively. The $BaTiO_3$ layer is grayish while the MgO and 90M10B layers are dark. The layers are well defined with straight interfaces, and no residual porosity can be observed on the interfaces. The interface layers were firmly bonded so that no delamination occurred even during the cutting and grinding operations for machining the specimens.

It was found that a crack easily developed perpendicular to the $BaTiO_3$/MgO interface of the specimen (as shown in Fig. 8). Since the difference of the thermal expansion coefficients between $BaTiO_3$ and MgO, with a value of $14\times10^{-6}$/K and $15.3\times10^{-6}$/K for $BaTiO_3$ and MgO, respectively [1], one origin of the residual stress is the thermal expansion mismatch of the different phases. Biaxial tensile stress in the layer was expected with the higher thermal expansion. Microcracking and the thermal stresses were also found in multilayered HA-Zirconia composites, which were prepared by SPS [4]. By means of a two step sintering method, the MgO pre-sintered

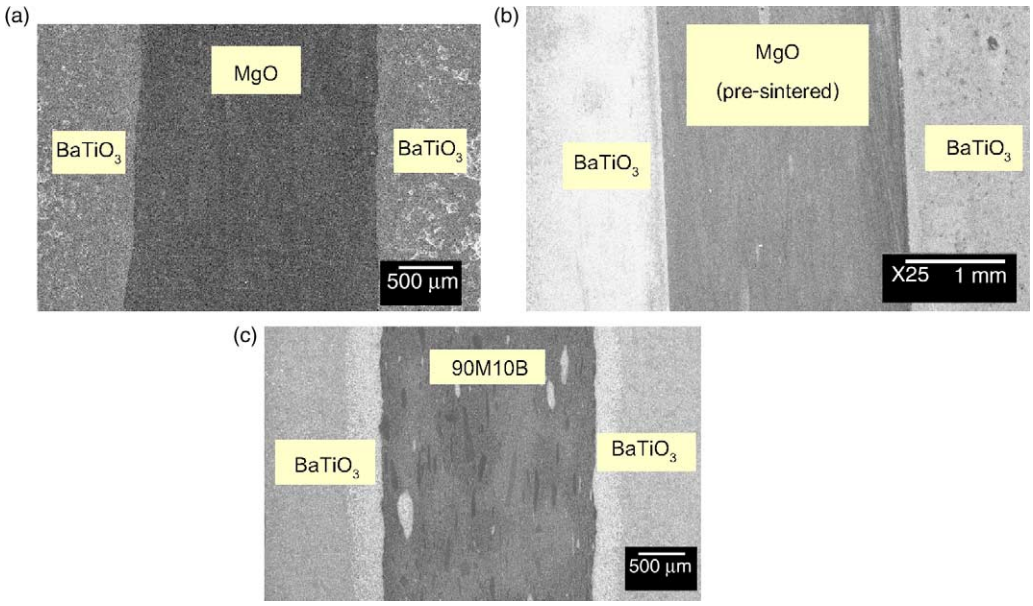


Fig. 7. Microscopic photographs of the cross-sections of (a) $BaTiO_3$/MgO/$BaTiO_3$, (b) $BaTiO_3$/MgO(pre-sintered)/$BaTiO_3$ and (c) $BaTiO_3$/90M10B/$BaTiO_3$ laminates.

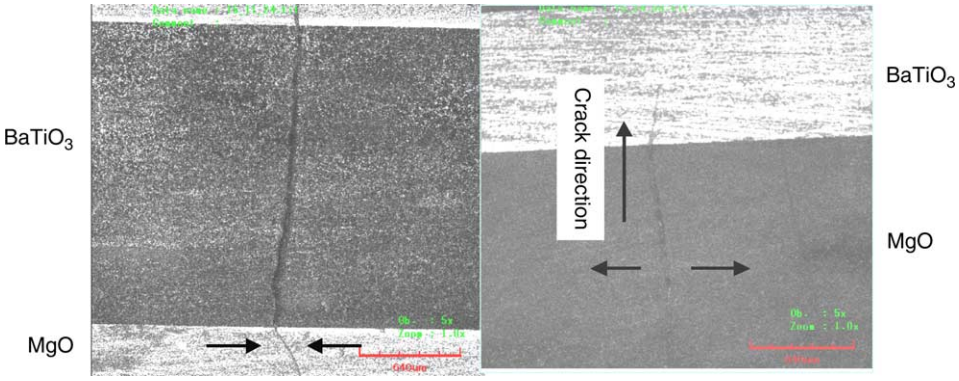


Fig. 8. Crack formed inside the MgO layer for $BaTiO_3$/MgO/$BaTiO_3$ laminate.

layer was stacked with both sides by $BaTiO_3$ layers and sintered again. The tensile crack was avoided and $BaTiO_3$/MgO (pre-sintered)/$BaTiO_3$ was successfully fabricated. $BaTiO_3$/90M10B/$BaTiO_3$ were fabricated and no crack was found.

A micro-compositional analysis of the interface was performed using EDS at an accelerating voltage of 20 kV. The results of the EDS line analysis of $BaTiO_3$/MgO/$BaTiO_3$ and $BaTiO_3$/MgO (pre-sintered)/$BaTiO_3$ laminates are shown in Fig. 9 (a) and (b), respectively. It was found that no reaction occurred between $BaTiO_3$ and MgO at the interface. Fig. 9 (c) also shows no reaction at the interface between the $BaTiO_3$ and 90M10B layers.

### *3.4. Voltage response under fatigue loading for poled $BaTiO_3$/MgO/$BaTiO_3$ laminate without cracking*

Fig. 10 shows the voltage response related to the cyclic stress for a poled $BaTiO_3$/MgO/$BaTiO_3$ laminate specimen without a crack, as compared to that of the poled $BaTiO_3$. The voltage response is positive when tensile stress is applied while it becomes negative when compressive stress is applied. This indicates that the present laminate exhibits strain sensing.

### *3.5. Effect of maximum stress on the voltage response range of the poled $BaTiO_3$ without cracking*

The voltage response range was determined by the range between maximum and minimum of voltage response of poled laminate specimen under a fatigue test. The voltage response of poled $BaTiO_3$ was recorded at different maximum stress levels during a fatigue test. The responding output range was determined from the range between maximum and minimum of responding output voltage. The results are shown in Fig. 11. The voltage response range increased with increasing maximum stress level up to 34 MPa. With further increase in maximum stress, the voltage response range was reduced. This may result from the fact that at higher stresses domain switching is exhausted and cannot take place any further. Calderon et al. [10,11] investigated the behavior of hard PZT under cyclic mechanical loading. The mechanical stressing induced irreversible deformation by the irreversible switching of 90° domains [10]. Cyclic loading initially produced a significant amount of cumulative irreversible strain on each cycle before eventual saturation. They suggested that the stress-induced domain switching behavior of PZT had

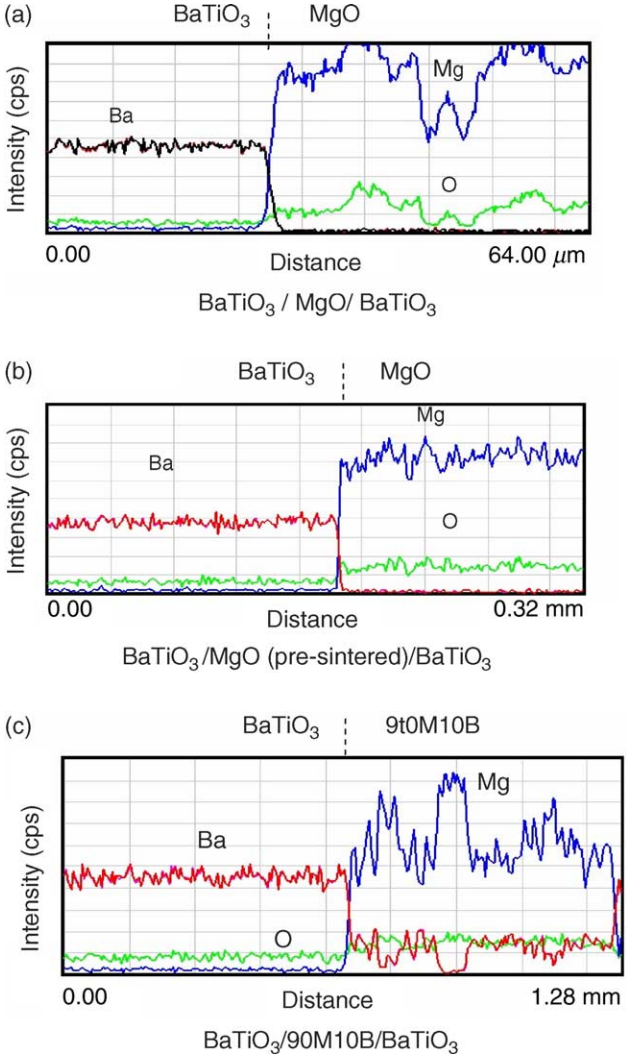


Fig. 9. EDS line analysis of the near interface region of laminates.

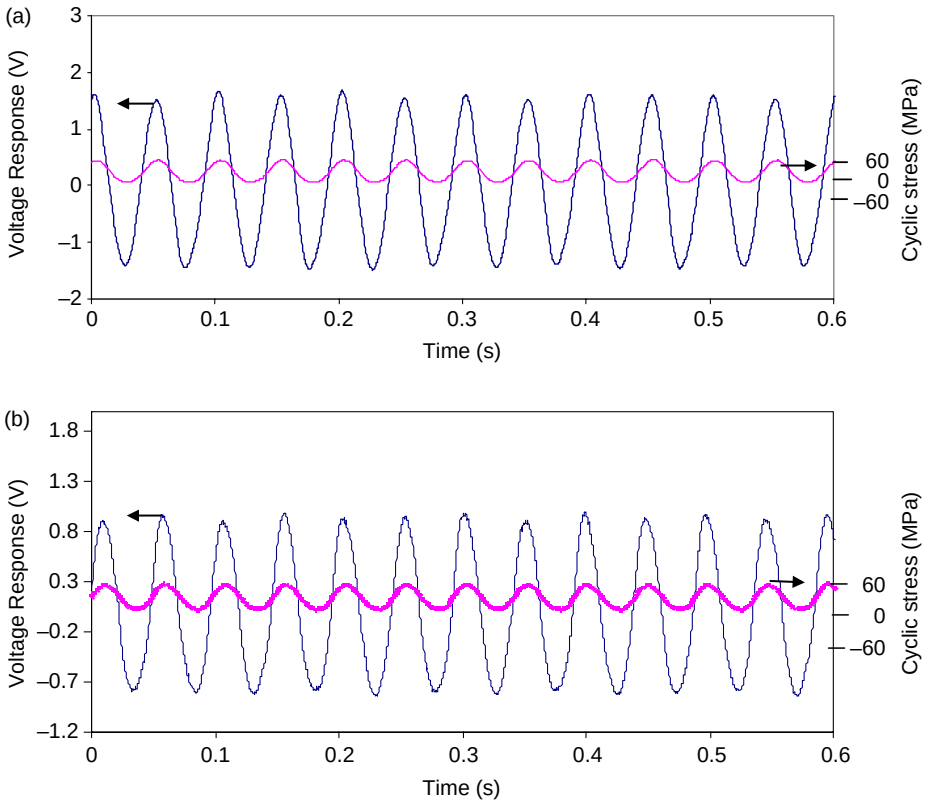


Fig. 10. The voltage response related to cyclic stress during a fatigue test for (a) poled $BaTiO_3$ and (b) poled $BaTiO_3$/MgO/$BaTiO_3$ without crack.

a saturated value of permanent cyclic strain with a strong dependence on maximum cyclic load [11]. The irreversible strains are produced by the domains that remain permanently reoriented, and resulted in de-poling and degradation of the piezoelectric properties. For the monolithic $BaTiO_3$ in this study, the number of reversible domains was reduced when the higher maximum stress of 34 MPa was applied, and consequently the voltage response range decreased.

### *3.6. Relationship between the voltage response range and crack length*

Fig. 12 shows the relationship between the voltage response range and crack length for the monolithic and the laminates. For the present monolithic $BaTiO_3$ and the laminates, the voltage response range decreased with increasing crack length. The slopes were generally similar regardless of the materials.

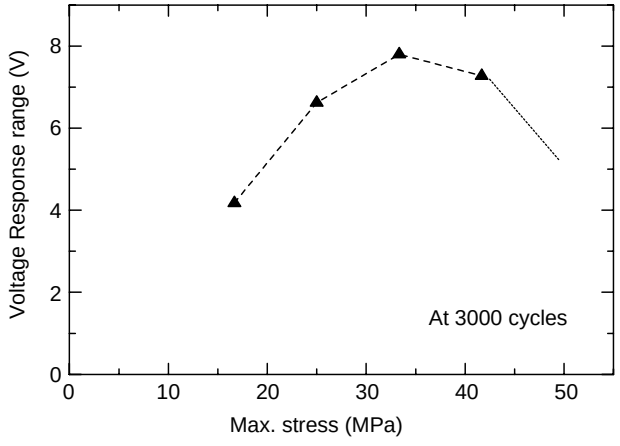


Fig. 11. Relationship between maximum stress and the voltage response range for poled $BaTiO_3$.

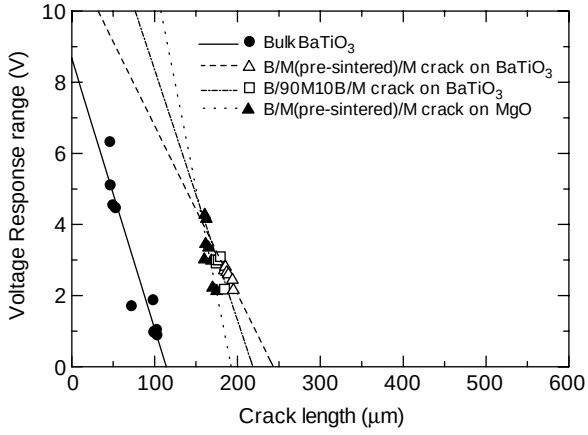


Fig. 12. Relationship between crack length and the voltage response range.

Due to the residual tensile stress in the MgO layer of the $BaTiO_3$/MgO/$BaTiO_3$ laminate, a crack in the MgO layer was propagated quickly and reached the $BaTiO_3$ layer immediately. On the contrary, a crack in the MgO layer was propagated perpendicular to the poling direction, in which the fracture toughness was lower than another direction.

Ferroelectric ceramics exhibit *R*-curve behavior [12–14]. It is believed that the main mechanism for increasing resistance with crack growth in ferroelectrics is similar to that in materials with transformation toughening. A process zone develops ahead of the crack tip, where high tensile stress causes ferroelastic domain switching [15]. As a crack propagates, residual compressive stress develops in the crack wake, and reduces tensile stresses at the crack tip (so-called crack tip stress shielding). Many studies have been carried in order to understand ferroelectric fatigue behavior and many corresponding mechanisms have been suggested. Ferroelastic domain switching in the vicinity of cracks in soft-PZT was examined by X-ray microdiffraction [16]. The fatigue properties of PLZT ferroelectric ceramic under alternate electric field were investigated [17]. During the fatigue process, switchable polarization of the ferroelectric sample decreased with increasing accumulative switching of ferroelectric polarization. Based on the image of diffracted X-ray radiation using a position sensitive detector, ferroelastic domain switching during fracture of PZT ceramics was studied [18]. X-ray diffraction provides direct quantitative information about the distribution of domains with different crystallographic orientations, and the high spatial resolution of the detector provides an accurate determination of domain switching within small areas of the sample. It was shown that the high spatial resolution of the detector allowed accurate measuring of the spatial distribution of the domain switching near the fracture. The present results can be explained accordingly: during crack propagation, the irreversible domain switching occurs in the crack wake and then causes the degradation of piezoelectric properties.

## 4. Conclusion

The SPS process was applied the fabrication of $BaTiO_3$/MgO/$BaTiO_3$ and $BaTiO_3$/90M10B/$BaTiO_3$ laminates. $BaTiO_3$/MgO/$BaTiO_3$ laminate could not be sintered from the compact of three layered powders because cracks were formed perpendicular to the interface in the MgO layer. With a pre-sintered MgO piezoelectric layer and $BaTiO_3$ powder layers, the laminate was successfully sintered. From the EDS line analysis, no reaction between $BaTiO_3$, MgO and 90M10B layers was observed along the interface. The responding output signal from the $BaTiO_3$ surface layer could be detected under cyclic loading.

The fatigue characteristics of $BaTiO_3$/MgO (pre-sintered)/$BaTiO_3$ and $BaTiO_3$/90M10B/$BaTiO_3$ laminates have been investigated. During the fatigue test, the voltage response indicated a clear correlation with the applied stress for monolithic $BaTiO_3$ and the laminates. With increasing applied stress, the voltage response range increased for monolithic $BaTiO_3$. Above the maximum stress of 34 MPa, the voltage response range decreased. It indicated that high mechanical stress could degrade the piezoelectric property by inducing irreversible switching of 90° domains. The voltage response range decreased with increasing crack length. The slopes of the relationship between the voltage response range and crack length were generally similar regardless of the materials. Therefore, it can be concluded that the laminates developed in the present study have a capability for sensing crack growth.

## Acknowledgements

The authors would like to thank Macoh Co., Ltd providing help with the use of a SPS machine. The present research was supported by the 21st century COE program, Ministry of Education, Culture, Sports, Science and Technology, Japan.

## References

[1] D. Munz, T. Fett, Ceramics: Mechanical Properties, Failure Behavior, Materials Selection, Springer, Berlin, 1999.
[2] B. Jeff, W.R. Cook, H. Jaffe, Piezoelectric Ceramics, Academic Press, London, 1971.
[3] T. Nagai, H.J. Hwang, M. Yasuoka, M. Sando, K. Niihara, Preparation of a barium titanate-dispersed-magnesia nanocomposites, J. Am. Ceram. Soc. 81 (2) (1998) 425–428.
[4] X.M. Chen, B. Yang, A new approach for toughening of ceramics, Mater. Lett. 33 (1997) 237–240.
[5] B. Yang, M. Chen, Alumina ceramics toughened by a piezoelectric secondary phase, J. Eur. Ceram. Soc. 20 (2000) 1687–1690.
[6] S. Rattanachan, Y. Miyashita, Y. Mutoh, Microstructure and fracture toughness of a spark plasma sintered $Al_2O_3$-based composite with $BaTiO_3$ particulates, J. Eur. Ceram. Soc. 23 (2003) 1269–1276.
[7] H. Gao, K.A. Khor, Y.C. Boey, X. Miao, Laminated and functionally graded hydroxyapatite/yttria stabilized tetragonal zirconia composites fabricated by spark plasma sintering, Biomaterials 24 (2003) 667–678.
[8] A.S. Shaikh, R.W. Vest, M. Vest, Dielectric properties of ultrafine grained $BaTiO_3$, IEEE Trans. Ultrason., Ferro Freq. Contro. 36 (4) (1989) 407–412.
[9] W. Luan, L. Gao, H. Kawaoka, T. Sekino, K. Niihara, Fabrication and characteristics of fine-grained $BaTiO_3$ ceramics by spark plasma sintering, Ceram. Int. 30 (2004) 405–410.
[10] Z. Shen, M. Johnsson, M. Nygren, TiN/$Al_2O_3$ composites and graded laminates thereof consolidated by spark plasma sintering, J. Eur. Ceram. Soc. 23[7 (2003) 1061–1068.
[11] J.M. Calderon, F. Moreno, M. Guiu, M.J. Reece, M.c.N. Alford, S.J. Penn, Anisotropic and cyclic mechanical properties of piezoelectric compression testing, J. Eur. Ceram. Soc. 19 (1999) 1321–1324.
[12] J.M. Calderon, M. Popa, Stress dependence of reversible and irreversible domain switching in PZT during cyclic loading, Mater. Sci. Eng. A336 (2002) 124–128.

[13] S. Baik, M. Lee, R-curve behavior of PZT ceramics near the morphotropic phase boundary, J. Mater. Sci. 29 (1994) 6115–6122.
[14] F. Meschke, O. Raddatz, A. Kolleck, A. Schneider, R-curve behavior and crack-closure stresses in barium titanate and (Mg,Y)-PSZ ceramics, J. Am. Ceram. Soc. 83 (2000) 353–361.
[15] K. Mehta, A. Virkar, Fracture mechanisms in ferroelectric-ferroelastic lead zirconate titanate (Zr:Ti =0.54:0.46) ceramics, J. Am. Ceram. Soc. 73 (1990) 567–574.
[16] S. Hackemann, W. Pfeiffer, Domain switching in process zones of PZT: characterization by microdiffraction and fracture mechanical methods, J. Eur. Ceram. Soc. 23 (2003) 141–151.
[17] N. Zhang, L. Li, Z. Gui, Non-destructive investigation of microstructure evolution due to ferroelectric fatigue in PLZT ceramics, Mater. Lett. 56 (2002) 244–247.
[18] A.E. Glazounov, J. Hoffmann, Investigation of domain switching in fractured ferroelectric ceramics by using imaging of X-ray diffraction, J. Eur. Ceram. Soc. 21 (2001) 1417–1420.